

Failure Mechanics of Low Velocity Dynamic Impact on Woven Polymeric Composites in Arctic Conditions



Pavana Prabhakar

1 Introduction

The rise and demand in arctic exploration has necessitated an in-depth understanding of the mechanical behavior and failure mechanisms of materials exposed to arctic conditions. Structures in such applications are often subjected to adverse environments like sea water, wave impacts or extreme low temperatures, which can cause surface alterations, internal damage, and degradation of chemical and mechanical properties that may ultimately compromise the safety of the naval structure. Therefore, the materials used in these structures must be able to withstand harsh environmental conditions of extreme low temperatures in addition to mechanical loads. Fiber reinforced polymeric composite (FRPC) have become an attractive option for this type of applications due to their corrosion resistance, high strength-to-weight ratio, ability to absorb noise and vibration damping, ease of fabrication, maintenance and repair [10, 18, 38]. They have been successfully integrated in offshore applications such as offshore vessels, ships hulls, tanks or pipes [16, 39]. Despite several advantages that FRPCs offer, a major drawback is their low resistance to impact damage due to their layered nature. Therefore, the motivation of this paper is to investigate the influence of combined arctic temperature ($-50\text{ }^{\circ}\text{C}$) and low-velocity singles and repeated impact loading on the damage and failure mechanisms of woven carbon/vinyl ester laminates.

Dynamic impacts on structures can occur under several different scenarios, including but not limited to, tool drop during maintenance and repair, hail strikes, iceberg collision, wave slamming [13, 25, 47], etc. These impacts are divided into low- and high-velocity. Low-velocity impacts typically occur at velocities below

P. Prabhakar (✉)

Civil & Environmental Engineering, Engineering Physics (Affiliate),
University of Wisconsin – Madison, Madison, WI, USA
e-mail: pavana.prabhakar@wisc.edu

© Springer Nature Switzerland AG 2020

S. W. Lee (ed.), *Advances in Thick Section Composite and Sandwich Structures*,
https://doi.org/10.1007/978-3-030-31065-3_20

579

10 m/s [42], which may produce barely visible damage (BVD) on composite surfaces, but with the possibility of significant internal damage. This is deemed very dangerous, as BVD could result in catastrophic failure of the structure without warning. The energy ranges vary between applications, but the velocities are maintained below 10 m/s [13, 25, 47]. The impact energies were chosen in the current paper based on the work presented by previous researchers. Common failure modes observed during low-velocity impacts are matrix cracking, fiber breakage and delamination [1, 9, 35]. Of these, delamination is one of the most common failure mechanisms [44], which often results in the reduction of stiffness, strength, durability and stability of composites [5, 40].

To establish the life and durability of FRPC in arctic conditions, in-depth investigation into the influence of combined impact and low temperature needs to be conducted. In real applications, structures are not impacted once, but are constantly subjected to repeated impacts like in the case of wave impacts, main shut-down of an off-shore platform, drifting supply vessels or ice impacts [19, 24]. Most of the previous impact studies have focused on single low-velocity and repeated impact at room temperature. Naik et al. [32] investigated the damage imparted to woven-fabric and cross-ply E-glass/epoxy and carbon/epoxy laminates under low-velocity (1 m/s and 3 m/s) impact. They reported that woven-fabric laminates were more resistant to in-plane impact damage than cross-ply laminates. Rajkumar et al. [34] studied the effect of repeated low-velocity impacts on glass fiber metal composites, and established that the peak load, impact energy, and failure strain decreased with increasing number of impacts. Sayer et al. [37] investigated the impact response of hybrid composite plates (glass-carbon/epoxy) with different stacking sequence for impact energies ranging between 25–75 J, and concluded that fiber fracture was the dominant failure mode as the impact energy increased.

Murat et al. [31] tested woven carbon/epoxy prepreg laminates at different impact energy levels in the range of 1 J – 10 J, and observed that thicker samples manifested higher resistance to impact damage and the damage area increased with increasing impact energies. Morais et al. [30] investigated the effect of repeated low energy impact response of carbon-epoxy composites with different stacking sequences, and reported that cross-ply and non-symmetric laminates have better endurance against low energy impacts than unidirectional laminates. Li et al. [27] studied the influence of the thickness of carbon fiber composites under low-velocity impact with energies of 17 and 18 J, and reported that the contact force, absorbed energy and bending stiffness decreases with reducing sample thickness. Nguyen et al. [33] investigated the influence of low, medium and high velocity impact on carbon fiber reinforced polymeric composites with impact energies of 10 J, 40 J and 120 J, respectively. They reported that the predominant damage mode was minor delamination, large delamination and fiber fracture and perforation, corresponding to low, medium and high velocity impact, respectively. Sultan et al. [43] studied woven carbon fiber reinforced prepreg laminates with impact energies ranging between 0.4–42 J, and reported that matrix cracking occurred below 21 J and fiber breakage manifested at energies between 21–31 J.

Despite an extensive amount of research conducted at room temperature (RT) under single and repeated impact loading, seldom work has been reported on repeated impact in arctic temperatures (AT). Icten [22] studied the influence of temperature on single and repeated impact of woven glass-epoxy composites at room temperature and $-50\text{ }^{\circ}\text{C}$. They observed that the laminates impacted at $-50\text{ }^{\circ}\text{C}$ recorded higher peak forces and absorbed less energy than the samples impacted at room temperature. Ibekwe et al. [21] investigated the impact response of glass fiber reinforced unidirectional and cross-ply laminated composite beams at $20\text{ }^{\circ}\text{C}$, $10\text{ }^{\circ}\text{C}$, $0\text{ }^{\circ}\text{C}$, $-10\text{ }^{\circ}\text{C}$ and $-20\text{ }^{\circ}\text{C}$, and observed that more damage was induced in the specimens impacted at lower temperature than those at higher temperatures. Salehi-Khojin et al. [36] investigated three combinations of fiberglass and Kevlar woven composites. Three different impact energies were tested (8 J, 15 J, and 25 J) for temperatures ranging from $-50\text{ }^{\circ}\text{C}$ to $120\text{ }^{\circ}\text{C}$. They reported that the deflection, maximum force and energy absorption increases with increasing temperature (from $-50\text{ }^{\circ}\text{C}$ to $120\text{ }^{\circ}\text{C}$) and impact energy (from 8 J to 25 J). Lopez-Puente et al. [29] investigated the influence of low temperatures on the damage imparted in carbon fiber/epoxy laminates (tape and woven) by impact velocities ranging from 60 to 525 m/s and at three temperatures (25, -60 and $-150\text{ }^{\circ}\text{C}$). They reported that higher kinetic energy and low temperature resulted in larger damage in the laminates. In addition, they concluded that as the velocity increased, damage saturation occurs and temperature will not influence the damage extension. Im et al. [23] investigated the effect of different temperatures (-30 , 20, 90 and $120\text{ }^{\circ}\text{C}$) on carbon fiber/epoxy and carbon fiber/peek laminates with lay-up $[0_6/90_6]_s$ and $[0_4/90_4]_s$. They concluded that as the temperature increases, the delamination areas decrease. Gomez-del-Rio et al. [17] recorded the response of carbon fiber reinforced polymeric composites with different stacking sequences (unidirectional, cross-ply, quasi-isotropic and woven laminates) in ambient temperatures ranging from $20\text{ }^{\circ}\text{C}$ to $-150\text{ }^{\circ}\text{C}$. They reported that the extent of damage and absorbed energy increased with the decrease in temperature for all tape laminates, however, woven laminates did not exhibit this trend.

There have been mixed observations with respect to the extent of damage under low-velocity impact loading at low temperatures for composites and seldom work has been reported on low-velocity repeated impact on carbon fiber reinforced polymeric composites. Therefore, in the current study, the response and failure mechanisms of woven carbon/vinyl ester laminates subjected to low-velocity single and repeated impact loading at room ($25\text{ }^{\circ}\text{C}$) and arctic temperature ($-50\text{ }^{\circ}\text{C}$) for a range of impact energies are investigated. Vinyl ester is considered in the current study due to superior UV resistance and low water absorption as compared to polyester resins [28, 41], which makes it attractive for ship and offshore applications. The variations in impact response in terms of force, displacement, energy and damage mechanisms is studied in detail and presented here.

2 Experimental Procedures

2.1 Manufacturing

Carbon fiber laminates were fabricated using vacuum assisted resin transfer molding (VARTM) process. Material system, fabrication process and sample dimensions used in this study are discussed next.

2.1.1 Material System

3 K tow (3000 filaments per tow) plain weave carbon fiber fabrics were used to manufacture the laminates investigated in this paper. These fabrics typically create lightweight and tensile stiffened structural products, and are also compatible with a variety of thermoset and thermoplastic resins. This type of fabric is commonly used in aerospace, marine and automobile applications. Hetron 922 vinyl ester resin, formulated for 1.25% MEKP hardener, was the resin system used for impregnating the dry carbon fabric during the VARTM process. Hetron 922 is a thermoset with low viscosity, which is advantageous for easy infiltration through the dry fabric during the VARTM process. Manufacturer provided mechanical properties of the carbon fibers and vinyl ester resin are given in Table 1.

2.1.2 Laminate Fabrication

Carbon fiber reinforced composite samples tested at 25 °C and –50 °C were manufactured by vacuum assisted resin transfer molding (VARTM) process [11]. Plain weave carbon fabric and vinyl ester resin were purchased from Fibre Glast (www.fibreglast.com). Laminates with 16 layers of dry fabric were manufactured according to the ASTM Standard D7136/D7136M [4]. The layers of fabric were placed between 2 layers of flow-media, 2 layers of breather and 4 layers of nylon peel ply. All layers were cut to dimensions of 305 mm × 305 mm. The arrangement of fabrics was placed between 2 aluminum molds, wrapped with Stretchlon 800 bagging film and sealed with vacuum-sealant tape, ensuring spaces for both inlet and outlet connectors (Fig. 1).

Table 1 Typical constituent material properties

Property	Carbon fiber	Vinyl-ester
Tensile strength	4.2–4.4 GPa	82.7 MPa
Tensile modulus	227.5–240.6 GPa	3.7 GPa
Elongation	1.4–1.95	4.6–7.9
Flexural strength	–	131 MPa
Flexural modulus	–	3.4 GPa
Nom. thickness	0.3048 mm	–

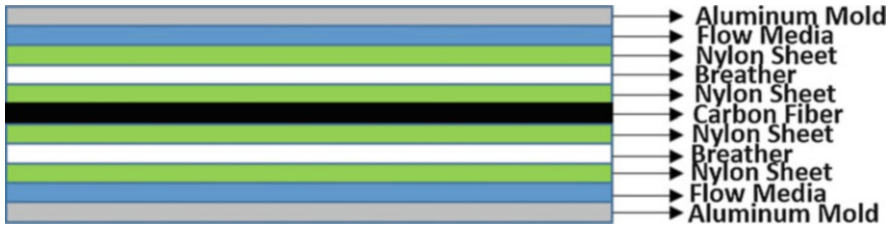


Fig. 1 Layer distribution of materials used in the VARTM process

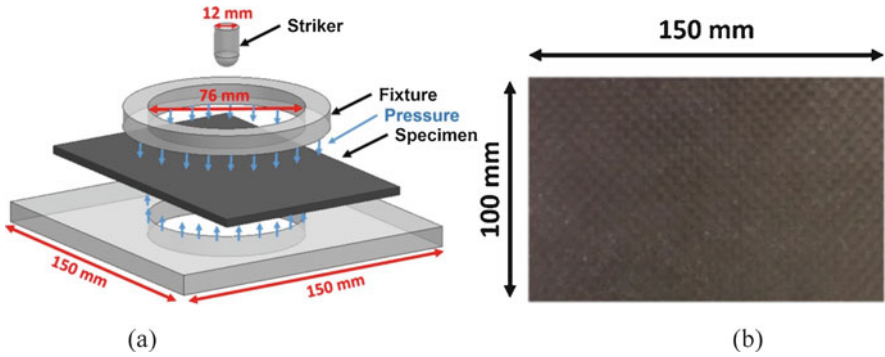


Fig. 2 (a) Dynamic impact fixture with striker; (b) Dimensions of impact sample

The woven dry fabrics were reinforced with a mixture of vinyl ester resin and Methyl Ethyl Ketone Peroxide (MEKP) hardener. The resin was catalyzed with 1.25% MEKP by weight and mixed thoroughly as recommended by the manufacturer. The resin/hardener mixture was placed in a desiccator first to remove bubbles from the mixture. The outlet was then connected to a vacuum pump until the vacuum bag achieved a pressure of approximately 80 MPa. The inlet of the vacuum bag was then submerged in the resin/hardener mixture for transferring resin through the laminate. Upon completion of the resin transfer process, the laminate was cured at room temperature for 24 h. A total of 6 plates of 305 mm length by 305 mm width were manufactured, and six samples were obtained from each plate. To ensure that the curing conditions were identical for all the samples at room and arctic temperature, half the samples from each plate fabricated were set for testing at 25 °C and the other half for -50 °C for a given impact energy.

2.2 Impact Tests

Drop-weight impact tests were performed using a CEAST 9340 Drop Tower Impact System on rectangular laminate samples of 150 mm length \times 100 mm width (refer to Fig. 2(b)) with an average thickness of 4.1 mm. The laminates were clamped

between two metal fixtures with a test area of 46 cm^2 as shown in Fig. 2(a). A hemispherical striker with a mass of 3.0 kg and diameter of 12.7 mm was used to impact the samples at their centers in the out-of-plane direction [4] with kinetic energies of 20 J, 25 J, 30 J, and 35 J for both temperatures ($25 \text{ }^\circ\text{C}$ and $-50 \text{ }^\circ\text{C}$). The impact velocity was calculated based on the mass of the striker and kinetic energy, using the equation, $E_k = \frac{1}{2} mv^2 = mgh$, where, E_k is the impact energy or kinetic energy, v is the impact velocity, m is the mass of the impacting striker, h is the height of the striker measured from the surface of a sample in the impact drop tower, and g is the gravitational acceleration.

For a particular impact energy (20 J, 25 J, 30 J or 35 J), the impact velocity and the striker falling height were adjusted accordingly by the Drop Tower Impact System, where the impact velocities were 3.64 m/s, 4.07 m/s, 4.46 m/s and 4.82 m/s, respectively. All the tests were low-velocity impacts, that is, below 10 m/s [8]. Single impact tests were conducted first. In order to establish the durability under repeated impact loading, each sample was repeatedly impacted until complete perforation of the striker through the sample thickness. Force-time, displacement-time and energy-time responses were recorded by the data acquisition system “CEAST DAS 8000 Junior” of the impact machine for each test. Schematic of an impact test fixture is shown in Fig. 2(a). Four samples were impacted for each combination of impact energy (20 J, 25 J, 30 J and 35 J) and temperature ($25 \text{ }^\circ\text{C}$ and $-50 \text{ }^\circ\text{C}$). Corresponding force-time, displacement-time, energy-time and force-displacement responses were obtained for each test.

The samples planned for testing under in-situ arctic conditions were placed in a Thermo Scientific™ freezer at $-50 \text{ }^\circ\text{C}$ for a period of 90 days to reach a uniform temperature. A basic heat transfer analysis was performed which showed that a sample at room temperature can $-50 \text{ }^\circ\text{C}$ in 15–20 min when subject to a constant ambient temperature of $-50 \text{ }^\circ\text{C}$. A 90 days exposure prior to testing was chosen to subject the samples to arctic pre-conditioning. To perform the in-situ arctic tests, the samples were removed from the freezer and placed within a temperature controlled environmental chamber, which was connected to the CEAST 9340 Drop Tower Impact System. Prior to every impact test, the environmental chamber was conditioned for 15 min with Liquid Nitrogen (LN_2) to reach a uniform temperature of $-50 \text{ }^\circ\text{C}$ within the chamber.

2.3 Quasi-Static Tests

To examine the strengthening effect of low temperatures, compression tests were performed on pure vinyl ester samples and tension tests were performed on woven carbon/vinyl ester samples at room and arctic temperatures. Compression Test: Three samples each of vinyl ester were tested at in-situ $25 \text{ }^\circ\text{C}$ and $-50 \text{ }^\circ\text{C}$ under flat-wise compressive loading. Cylindrical specimens with a diameter of 25.4 mm and a height of 50.8 mm were tested according to ASTM D695 standard [3]. These

tests were performed using an ADMET eXpert 1654 testing system with a crosshead displacement rate of 1.3 mm/min. Tension Tests: Five samples each were tested at in-situ 25 °C and -50 °C under tensile loading. Rectangular specimens with a width of 15 mm, thickness of 1 mm and length of 250 mm were tested according to ASTM D3039 standard [2]. These tests were performed using an ADMET eXpert 1654 testing system with a crosshead displacement rate of 2 mm/min.

2.4 *Micro Computed Tomography (micro-CT) Scanning*

Typically, low velocity impacts produce barely visible damage (BVD) on composite surfaces after a single impact. Hence, the samples were examined under a micro-computed tomography (micro-CT) scanner to evaluate the internal damaged regions in arctic and room temperature. The samples were reduced to a rectangle of 145 mm in length and 90 mm in width (the original dimensions were 150 mm in length by 100 mm in width), such that they can fit in the scanner chamber. The impact damage was centered in this rectangle and cutting around the edges did not alter the damage that occurred predominantly at the center of the samples and far away from the edges. A small hole with a diameter of 1.6 mm was drilled at the center of the impacted region of the laminates for applying a dye-penetrant at these holes, upon which the samples were held in a vacuum chamber for 5 min. This procedure was repeated three times to ensure that all damaged regions were filled with the solution. For the first 2 applications of the dye-penetrant, the solution was completely absorbed. A third application ensured that the sample was saturated with the solution, which resulted in complete solution penetration in all available openings, such as delamination and cracks. Zinc iodide solution was used as the dye-penetrant, which has a high absorption coefficient in comparison to the constituents of the composite materials i.e. carbon fiber and vinyl ester.

The Zinc iodide solution was a mixture of alcohol (10 ml), distilled water (10 ml), Kodak photo solution (1 ml) and zinc iodide powder (60 g). Excess dye-penetrant was evaporated by placing the laminates in an oven at 50 °C prior to x-ray scanning. Excess dye penetrant in its liquid phase is not preferred as its motion inside the crack during a scan adversely affects the quality of the 3-D reconstruction. This was eliminated through drying the dye penetrant, which deposits a saline residue on the crack area and in turn provides greater resolution of the damage. Hence, drying the dye penetrant is beneficial. Also, 50 °C is enough to dry the samples without creating any thermal damage in the composite. All laminates were scanned with a SkyScan 1173 X-ray micro-tomography with the same resolution of 35.9 μm and an angle step of 0.19. The X-ray tube voltage and current were set to 60 kV and 120 microampere, respectively. All the scans were performed using built-in Al filter, and a flat field correction was applied for each scan. The reconstruction was performed using the NRecon commercial software.

3 Results and Discussion

Deformation-time, energy-time and force-time responses recorded for impact energies of 20, 25, 30, and 35 J at 25 °C and –50 °C are discussed in detail in this section. Durability of laminates upon repeated impact is assessed in terms of number of impacts required to perforate a laminate through the thickness and the rate of reduction in the peak force for a combination of impact energies and temperatures. The response of the laminates in terms of visual damage, degree of damage and failure mechanisms is also evaluated and elucidated next.

3.1 Laminate Strengthening

Mechanical properties of woven carbon/vinyl ester composites change when cooled to arctic temperatures (AT). Prior research by Dutta [14] on the compressive response of glass-fiber-reinforced polymer composites at the U.S. Army Cold Regions Research and Engineering Laboratory (CRREL) showed that their strength and stiffness increases with reducing temperatures. But, also become brittle and are susceptible to cracks due to increase in thermal residual stresses caused by mismatch in the coefficient of thermal expansion (CTE) between the fibers and matrix.

3.1.1 Compression Test Results

Compression tests on pure vinyl ester were also conducted in-house as part of the current study to investigate the influence of low temperature on these composites. Table 2 shows the results from the compressive testing of vinyl ester, where the yield strength (coined as the stress value where the response starts to become non-linear), ultimate strength and elastic modulus increased by approximately 55%, 49% and 28% when cooled from 25 °C to –50 °C. Typical compressive stress-strain response (one sample) of vinyl ester is shown in Fig. 3, where the final failure strains reduced with reduction in temperature, which implies that deformation of vinyl ester will be lower at AT as compared to those at RT. The increase in matrix strength is attributed to the binding forces between molecules, which are tightly frozen at AT [12]. Therefore, the compressive strength of vinyl ester increases at low temperatures. Garcia et al. [15] investigated the flexural response of woven carbon/vinyl ester composites in AT, and reported that dry arctic conditioned samples manifested an $\approx 23\%$ increase in flexural strength with respect to those at room temperature.

Table 2 Results from compressive testing of vinyl ester at RT and AT

Mechanical properties	Temperatures (C)		Percentage change (%)
	25	–50 °C	
Yield strength (MPa)	47 ± 5	72 ± 4	55
Ultimate strength (MPa)	85 ± 4	126 ± 12	49
Elastic modulus (GPa)	2.6 ± 0.2	3.4 ± 0.1	28

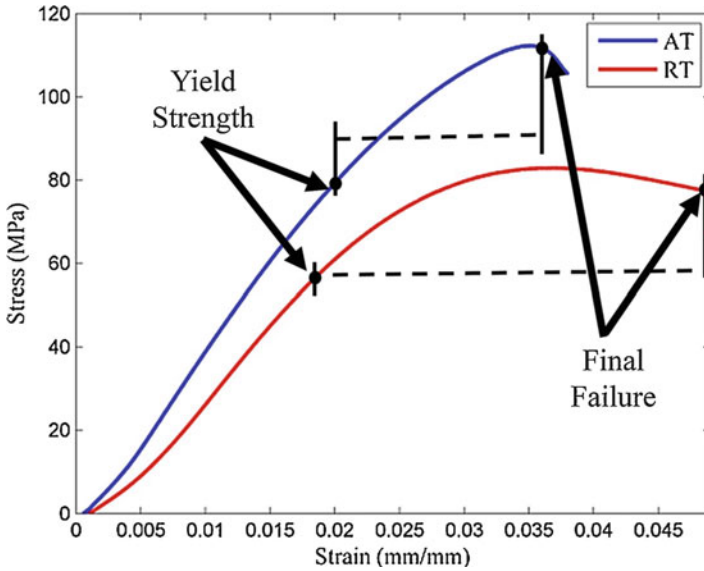


Fig. 3 Typical compressive stress-strain plots of vinyl ester at RT and AT

Table 3 Results from tensile testing of woven carbon/vinyl ester samples at RT and AT

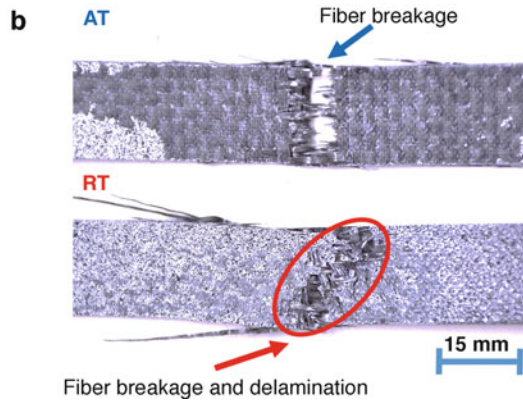
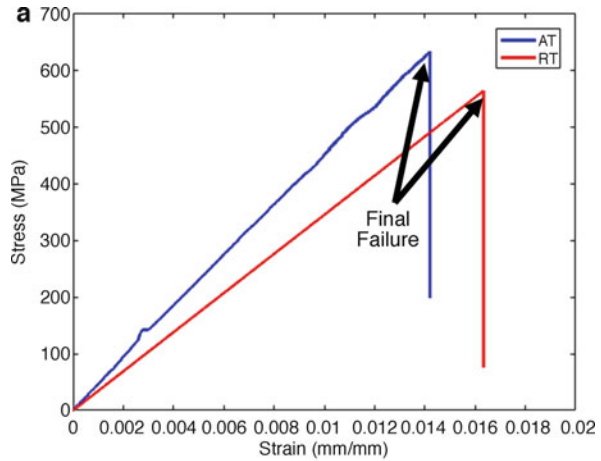
Mechanical properties	Temperatures (C)		Percentage change (%)
	25	-50 °C	
Ultimate strength (MPa)	562 ± 31	623 ± 29	11
Elastic modulus (GPa)	37 ± 4	42 ± 4	15

3.1.2 Tension Test Results

Tension tests on woven/carbon vinyl ester samples were also conducted in-house as part of the current study. Table 3 shows the results from the tensile testing of the woven carbon/vinyl ester composite, where the Young’s modulus and ultimate tensile strength increased by approximately 15% and 11% respectively when cooled from 25 °C to -50 °C. Typical tensile stress-strain response of woven carbon/vinyl ester is shown in Fig. 4(a), where the final failure strains reduce with reduction of temperature. This implied that there is a reduction of ductility and increase in brittleness of the composites at low temperature [20]. Kim et al. [26] attributed such increase in brittleness at low temperatures to predominantly fibers, which increased rapidly within a temperature range from RT to -50 °C.

On the other hand, the increase in the laminate strength and stiffness is attributed to the strengthening of the matrix. Therefore, there will be less damage at low temperatures initially, but it continues to increase as the load approaches a critical value where the fibers fail. However, matrix cracking and delamination will be dominant at room temperature [45]. Figure 4(b) shows the failure regions of one

Fig. 4 (a) Typical tension stress-strain plots of woven carbon/vinyl ester at RT and AT; (b) Failure regions of the composite specimens at RT and AT under tension



set of specimens tested at 25 °C and –50 °C under tension. It can be seen that at AT, the damage was localized in just one region (across the transverse direction of the sample) and fiber breakage was the dominant failure mechanism. On the other hand, the samples at RT experienced a more dispersed damage (across the longitudinal direction of the sample). In addition, matrix cracks and some fiber breakage were the main failure mechanisms. The samples at RT were painted white to show this failure pattern more clearly.

3.2 Contact Force and Deflection

During an impact test, contact force is generated by the contact of the striker with the impacted face of a sample, which is recorded as the force-time response by the data acquisition system of the impact machine.

3.2.1 Single Impact

Figure 5(a) shows a representative force-time graph of an impact event, where the maximum impact force corresponds to the peak value of the graph. Figure 5(b) shows the variation of maximum impact force for different impact energies for the specimens tested at room and arctic temperature. At both temperatures, the

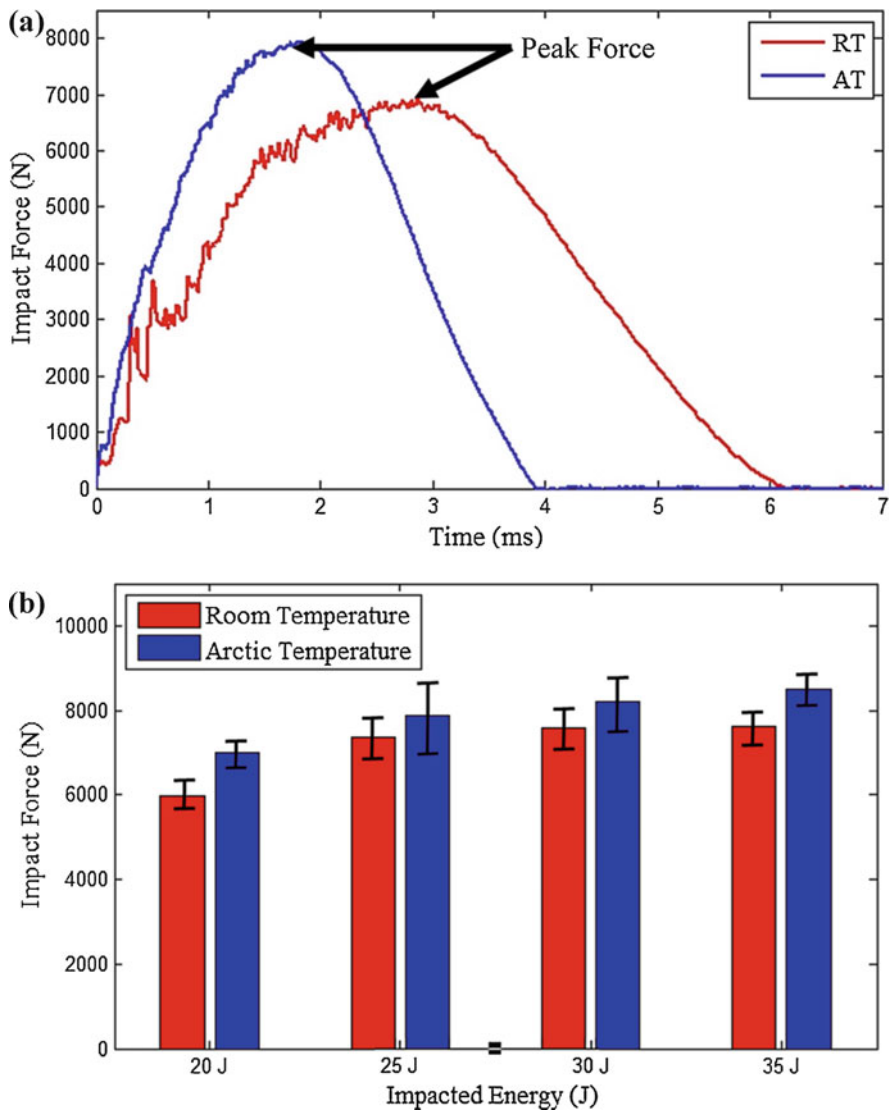


Fig. 5 (a) Representative force-time graph of an impact event at 20 J for RT and AT; (b) Impact contact force at RT and AT for 20 J, 25 J, 30 J and 35 J

maximum impact force increased with increasing impact energies. In addition, the specimens tested at AT experienced higher impact forces as compared to those tested at RT, which is attributed to the increase in strength of composites when subject to low temperatures as discussed in the section on “Laminate strengthening”. Also, laminates became stiffer at low temperatures rendering them less flexible as compared to those at room temperature.

The average initial slopes of the force-displacement responses for the samples tested at different impact energies for both temperatures is shown in Fig. 6, where the samples impacted at arctic temperature manifested higher stiffness values as compared to those at room temperature. This is attributed to the strength increase at low temperatures of the laminates. Due to the increased strength at arctic temperature, lower deflections were observed as compared to the samples tested at room temperature.

Figure 7 shows the deflection with varying impact energies. As expected, the deflections at both temperatures increased with the increasing impact energies.

3.2.2 Repeated Impact

Typical repeated impact responses of laminates impacted at two energies of 20 J and 25 J are shown in Figs. 8(a) and 8(b). In general, it is expected that the peak force recorded reduces with increasing number of impacts due to accumulation of damage. However, the specimens manifested two different responses at 20 J and 25 J. At 20 J, the peak forces increased initially upon repeated impacts, but reduced after several impacts finally resulting in perforation. At 25 J, the trend was as expected, where the peak force gradually reduces with increasing number of impacts.

Bienias et al. [7] categorized the repeated impact response into phases of force change. The first phase is called “stabilization”, represented by letter A in Fig. 8(a), which is the very first impact on a laminate where the impact energy is insufficient to cause damage for decreasing the stiffness of the laminate. Icten [22] attributes this to the contact of the impactor with a relatively compliant matrix material. The second phase is known as “force increase”, given by letter B in Fig. 8(a), which consists of multiple impacts before the maximum peak force is reached. In this phase, laminates experienced higher contact force after each impact due to the compaction of matrix under the striker. The third phase is “maximum force”, represented by letter C, which corresponds to the number of impacts at maximum peak force beyond which force reduction occurs due to the presence of damage, such as matrix cracks, fiber breakage and delamination. The last phase is “force decrease”, given by letter D, where the peak force and stiffness recorded gradually reduces with increasing number of impacts.

Specimens repeatedly impacted at 20 J at room and arctic temperatures manifested all four phases of force change (Fig. 8(a)), whereas, those impacted at 25, 30 and 35 J showed only phases C and D (Fig. 8(b)). Lower impact energies are not sufficient to damage the laminate in the first impact, thereby, causing phases A and B, as opposed to higher impact energies that manifest only phases C and D.

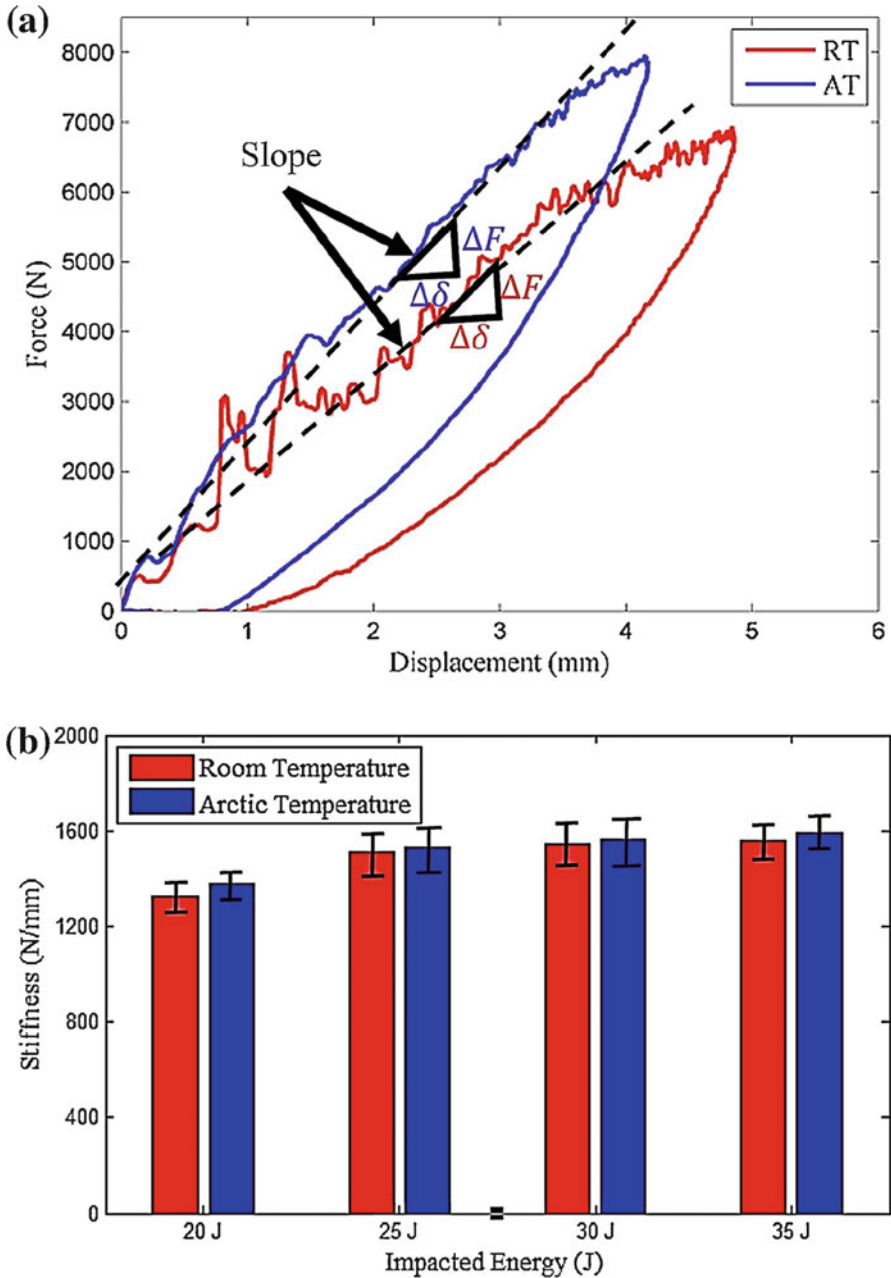


Fig. 6 (a) Representative force-displacement graph of an impact event at 20 J for RT and AT; (b) Stiffness (initial slope) at RT and AT for 20 J, 25 J, 30 J and 35 J

Fig. 7 Deflection for each impacted energy at room and arctic temperature

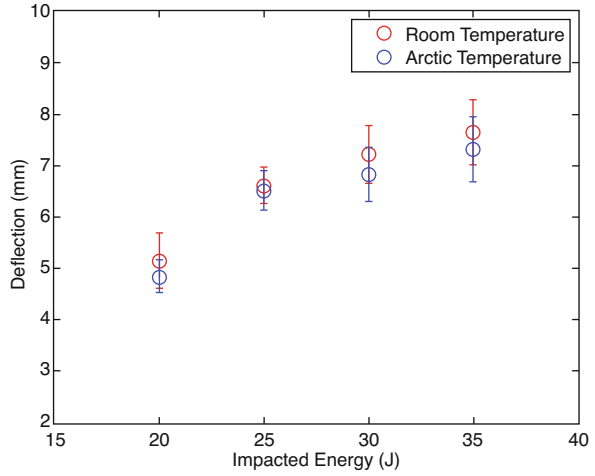
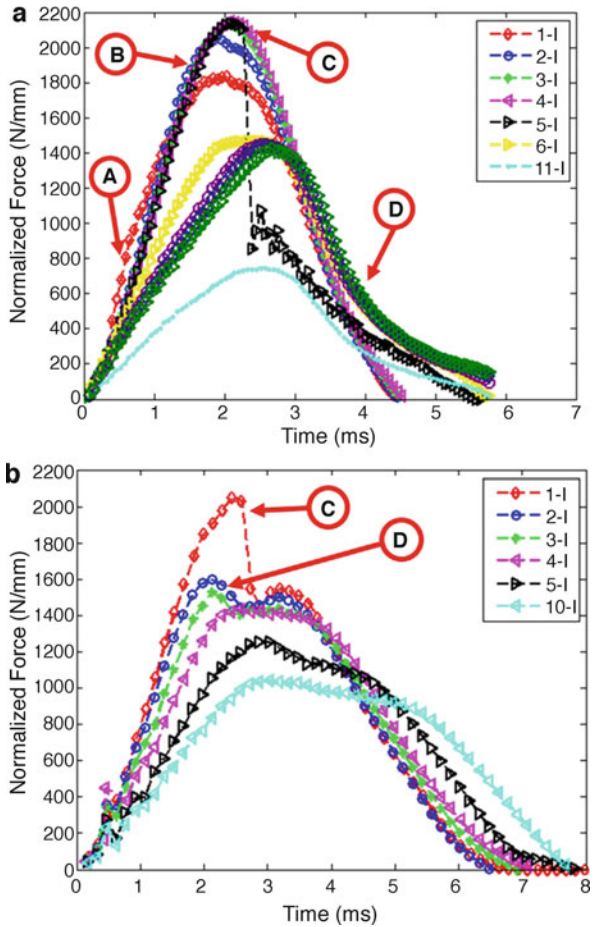


Fig. 8 Representative force-time responses for a single sample subject to repeated impact: (a) 20 J at arctic temperature; (b) 25 J at arctic temperature



3.2.3 Temperature Effect on Impact Force

Peak impact force is plotted against the number of impacts at room and arctic temperature in Fig. 9. For all energies, the samples impacted at $-50\text{ }^{\circ}\text{C}$ experienced higher impact forces and required a greater number of impacts to perforate the laminate as compared to the samples tested at $25\text{ }^{\circ}\text{C}$. The samples impacted at 20 J at both temperatures experienced the four phases of force change described above, which are, stabilization, force increase, maximum force and force decrease. Figure 9(a) shows the response for 20 J for both temperatures, where an increase in impact force after the first impact is observed corresponding to the force increase stage. Upon reaching a maximum impact force, a decrease in impact force is observed with further impacts. With increasing number of impacts, significant difference between the impact forces is observed at both temperatures. For 25, 30 and 35 J impact energies, the samples experienced only 2 phases of force change: maximum force and force decrease as shown in Figs. 9(b), 9(c) and 9(d).

The slope of the force versus number of impacts plot indicates the rate of reduction in impact force with increasing number of impacts, which is higher at

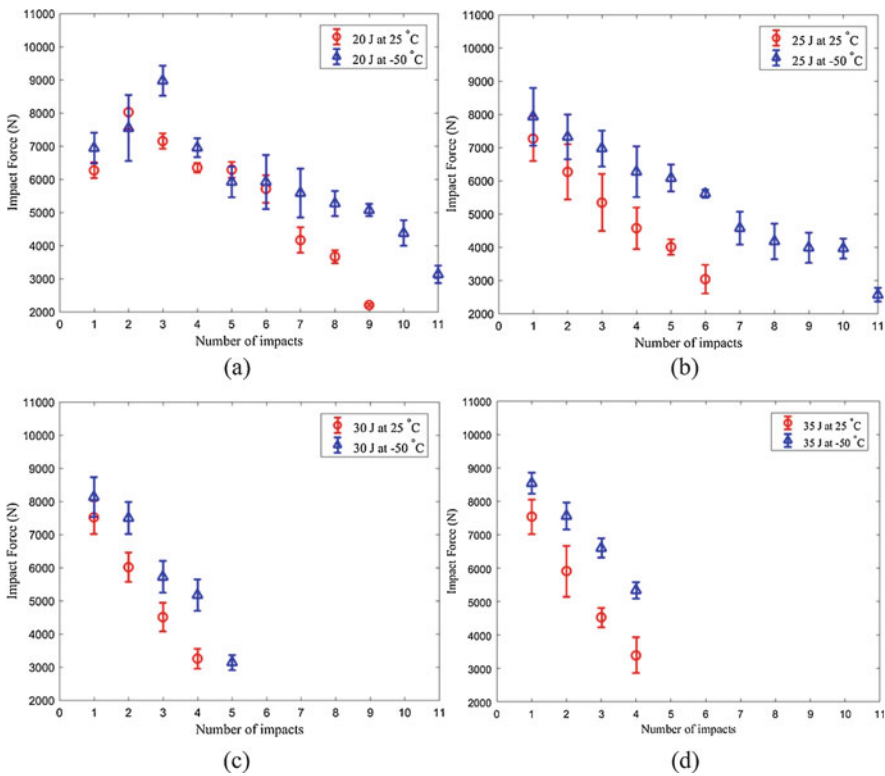


Fig. 9 Contact force with increasing number of impacts at $25\text{ }^{\circ}\text{C}$ and $-50\text{ }^{\circ}\text{C}$: (a) 20 J, (b) 25 J, (c) 30 J and (d) 35 J

higher impact energies of 30 J and 35 J, and also similar at room and low temperature. Fiber fracture is the dominant failure mechanism at higher impact energies as opposed to matrix cracking at lower impact energies. This is attributed to two factors: (1) lesser influence of low temperature on carbon fibers and damage saturation. The influence of low temperature on carbon fiber is less significant as compared to matrix, from what is observed in the case of coefficient of thermal expansion (CTE) [46]; (2) damage saturation occurs when the temperature has no influence on damage extension. This corroborates the similar responses at low and room temperature. As expected, the impact force at both temperatures increased with the increasing impact energy.

3.2.4 Temperature Effect on Deflection

Figure 10 shows the deflection versus number of impacts at room and arctic temperatures. Increase in rigidity of the laminates due to matrix strengthening at

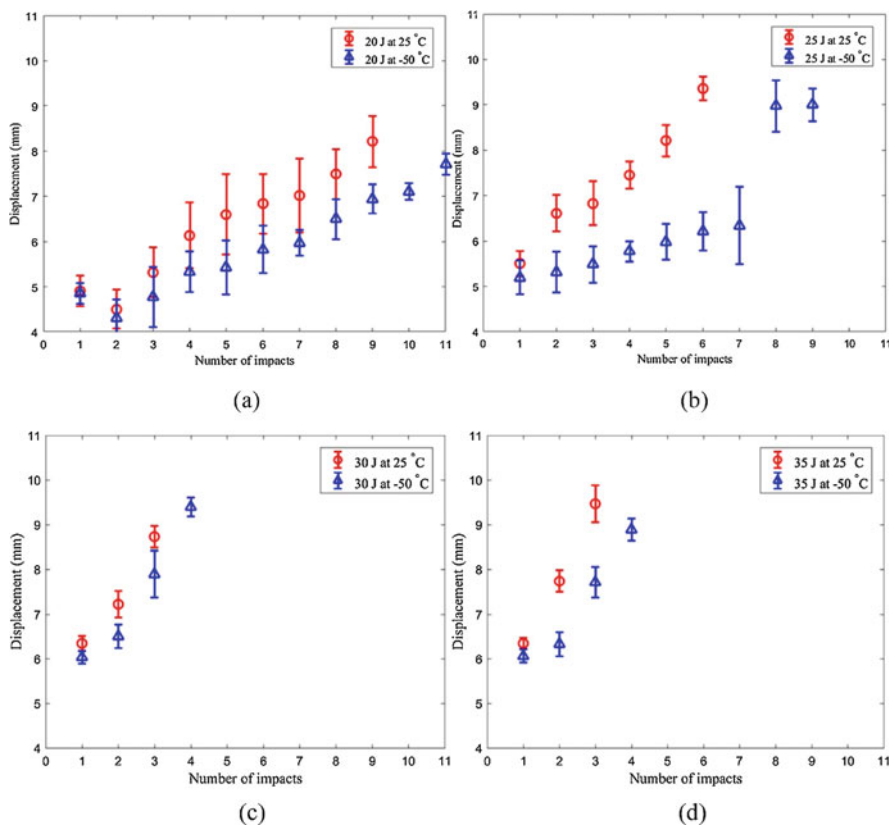


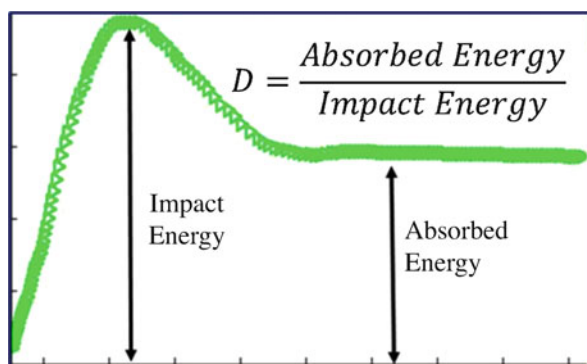
Fig. 10 Deflection with increasing number of impacts at 25 °C and -50 °C: (a) 20 J, (b) 25 J, (c) 30 J and (d) 35 J

arctic temperatures manifests lower deflections in samples impacted at $-50\text{ }^{\circ}\text{C}$ as compared to those at $25\text{ }^{\circ}\text{C}$. The deflection at both temperatures increased with the increasing impact energies. For 20 J (Fig. 10(a)) and 25 J (Fig. 10(b)), the difference between the deflections at room and arctic temperatures under repeated impact loading is more prominent, as compared to that observed for 30 J (Fig. 10(c)) and 35 J (Fig. 10(d)).

3.3 Absorbed Energy

Figure 11 shows a typical energy-time response obtained during an impact even on fiber reinforced laminates. The impacted energy is the peak value on the graph and the post peak plateau region is the energy absorbed by the laminate that is manifested as failure mechanisms like matrix cracking, delamination or fiber fracture. If the impact energy is equal to the absorbed energy, the laminate is deemed completely perforated by the strikers. Increasing absorbed energy implies more damage in the laminate. Hence, the degree of damage (D) for a laminate is defined as the ratio of the absorbed energy to the impact energy, which limits the values to be between 0 (no damage) and 1 (complete damage). The impacted laminates tested here were thin with an average thickness of $4 \pm 0.1\text{ mm}$. As a result, if the impact energy was equal to the absorbed energy, based on experimental observations, the laminates were deemed here to be completely perforated by the striker as a consequence of no rebound. However, in general, impact energy equals absorbed energy means that there is no rebound and all the impact energy is absorbed by the specimen typically as inelasticity or damage, which is especially true when the specimens are relatively thick or highly damping, in which case complete penetration is difficult to achieve. Increasing absorbed energy implies more damage in the laminate. Figure 12(a) shows representative energy-time graphs of the samples impacted at room and arctic temperature for 20 J, 25 J, 30 J and 35 J. In general, it is observed that the samples impacted at arctic temperature (blue color) absorbed less energy than the samples impacted at room temperature (red color).

Fig. 11 Typical energy-time response of an impact event



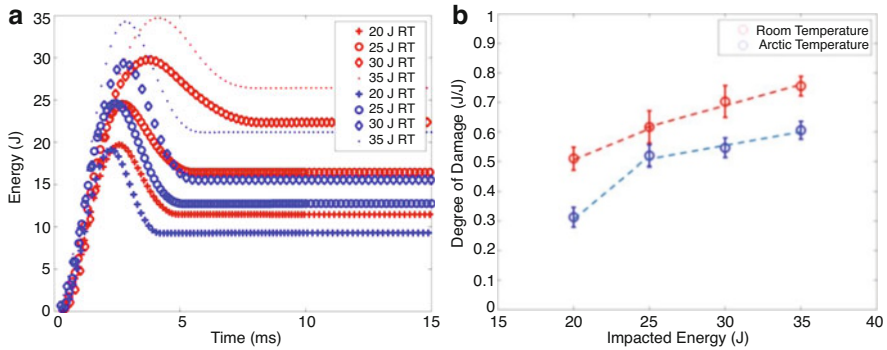


Fig. 12 (a) Representative energy-time graph for room (RT: 25 °C) and arctic temperatures (AT: −50 °C) at 20 J, 25 J, 30 J and 35 J, (b) Degree of damage for each impacted energy

To quantify the damage in the laminates, a term called degree of damage (D) coined previously by Belingardi and Vadori [6] was calculated, which is defined as the ratio between the absorbed energy and the impact energy. Figure 12(b) shows the degree of damage for different impact energies, where an increasing trend is observed with increasing impact energies. The samples impacted at AT recorded lower degree of damage as compared to the samples tested at RT for a specific impact energy, and is attributed to matrix strengthening at AT.

3.3.1 Single Impact

The trend lines in Fig. 12(b) show a knee formation at 25 J, below which the slope is higher than after. It is known that for fiber reinforced laminates, matrix failure is prevalent at lower impact energies and fiber failure is dominant at higher impact energies. Therefore, the contribution of matrix cracking at lower energies to the degree of damage is significant, whereas, a combination of fiber breakage and matrix cracking contributes at higher energies. However, due to matrix strengthening at AT, the damage in the matrix is lower than damage at RT at low impact energies as explained in the “Laminate strengthening” section. Therefore, the reduction in the degree of damage measured at 20 J between RT and AT is high, about 38% for these laminates. Whereas, at higher impact energies, that is above 25 J, this difference reduces (about 15–22% here) due to lower (but not insignificant) influence of matrix cracking on the degree of damage.

3.3.2 Repeated Impact

Figure 13(a) shows a representative energy-time graph for repeated impacts at 20 J, where the energy absorbed after the first impact (red) decreased first for the next

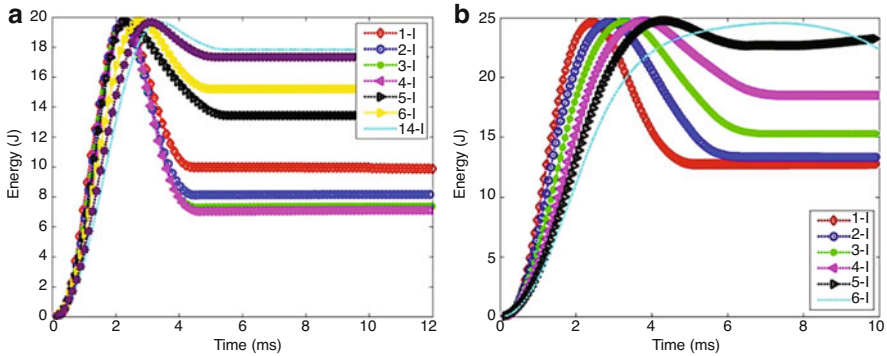


Fig. 13 Representative energy-time responses for repeated impact: (a) 20 J at arctic temperature; (b) 25 J at arctic temperature

three impacts (blue, green and magenta) due to the compaction of matrix during the “force change” phase as described before. Upon reaching the maximum force (black graph), there was a significant increase on the absorbed energy, which continues to increase gradually after consecutive impacts until laminate perforation. For 25 J, 30 J and 35 J, the energy absorbed increased gradually starting from the very first impact, as seen in Fig. 13(b).

3.3.3 Temperature Effect on the Degree of Damage Under Repeated Impact

Figure 14 shows the degree of damage versus number of impacts for room and arctic temperatures, where the values of D increase with increasing impact energies and also the number of impacts. In general, the samples impacted at $-50\text{ }^{\circ}\text{C}$ recorded lower degree of damage as compared to those at $25\text{ }^{\circ}\text{C}$ for a specific impact energy. The damage in matrix is lower at arctic temperature due to matrix strengthening than those at room temperature at low impact energies. It has been previously established that the matrix failure is prevalent at lower impact energies and fiber failure is dominant at higher impact energies. Therefore, the contribution of matrix cracking at lower energies to the degree of damage is significant, whereas, a combination of fiber breakage and matrix cracking contributes at higher energies. Therefore, the difference in the degree of damage measured at 20 J Fig. 14(a) and 25 J Fig. 14(b) between RT and AT is high, about 21–29% for these laminates. Whereas, at higher impact energies (Fig. 14(c) for 30 J and Fig. 14(d) for 35 J), this difference reduces to about 10–15% due to lower (but not insignificant) influence of matrix cracking on the degree of damage.

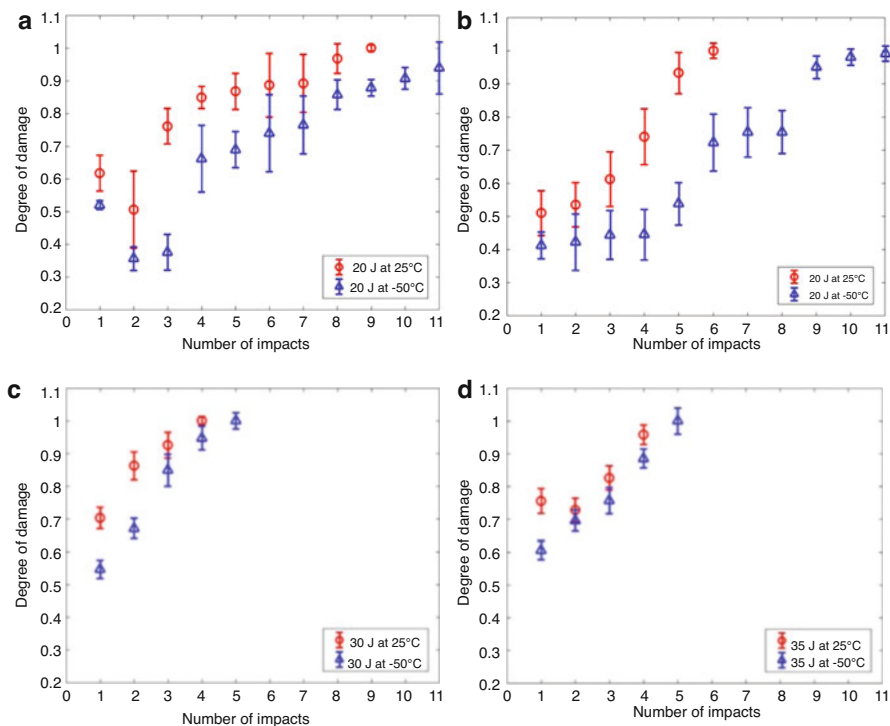


Fig. 14 Degree of damage as a function of number of impacts at 25 °C and -50 °C: (a) 20 J, (b) 25 J, (c) 30 J and (d) 35 J

3.4 Damage Mechanisms

3.4.1 Single Impact

Figure 15 shows the micro-CT scan images of samples impacted at 20 J and 30 J in room and arctic temperatures after a single impact. Regions identified as matrix cracking/delamination (smear areas) and fiber breakage (sharp defined areas) are highlighted in the images. From the images shown in Fig. 16, the samples impacted with 20 J energy at both temperatures manifested small regions of visible damage on the impacted and the back faces. However, the micro-CT scan images show considerable internal damage in terms of matrix cracking/delamination and fiber breakage through the thickness of the samples. Fiber breakage is concentrated on the impacted surface with significant matrix cracking and delamination through the thickness of the laminate impacted at 20 J energy in room temperature. On the other hand, at arctic temperature the overall spread of damage is confined to a smaller region with higher fiber failure traversing through the thickness of the laminate. The reduction in

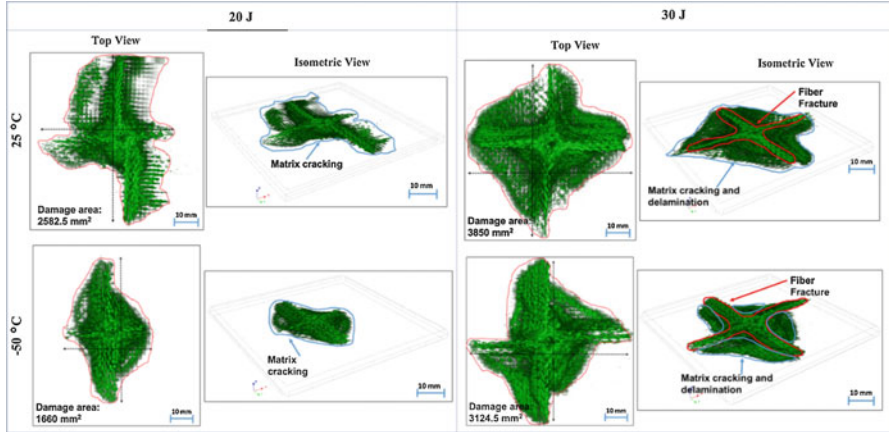


Fig. 15 Micro-CT scan after the first impact for 20 and 30 J at 25 °C and -50 °C

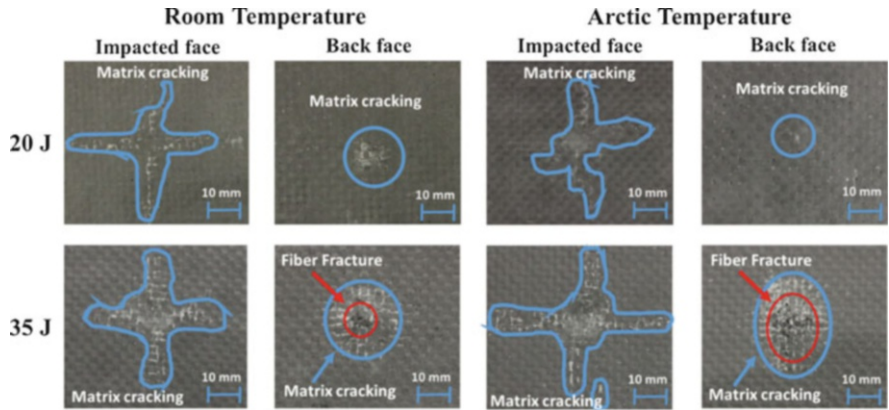


Fig. 16 Impacted face and back face at 20 and 35 J impact energies at 25 °C and -50 °C under single impact

the overall damaged area projected on to the plan of the samples is approximately 36% between RT and AT under 20 J of impact energy.

The micro-CT scan images for 30 J shown in the Fig. 15 exhibit significant fiber failure along with matrix failure, and is representative of the samples impacted at higher energies of 25, 30 and 35 J. Fiber failure through the thickness of the samples is higher at AT as compared to RT when impacted by 30 J impact energy. Also, the reduction in the overall damaged area projected on to the plan of the samples at 30 J is approximately 19% between RT and AT. The observed difference in percentage reduction in damaged area between RT and AT under 20 J and 30 J is due to the increase in strength when composites are subject to low temperatures. The yield strength of the vinyl ester matrix increased up to 55% at AT as compared to RT

based on the compression tests conducted in the current study, which indicates a delay in the onset of matrix cracks at AT. Consequently, the composite manifested significantly higher fiber failure than matrix cracking as compared to RT for the same impact energy.

Figure 16 shows the impacted face and back face of two samples after testing. The samples impacted at 20 J in room and arctic temperature did not exhibit fiber breakage, however, exhibited small regions of matrix cracking at the impacted and back face of the laminate as seen by the enclosed blue curves. On the other hand, the samples at 35 J exhibited a combination of fiber breakage (enclosed by the red circles) and matrix cracking at the back face in both temperatures. Even though the samples at 20 J did not exhibit a significant amount of visible damage externally, there was significant internal damage.

3.4.2 Repeated Impact

Figure 17 shows the impacted face and back face of samples repeatedly impacted at 20 J and 35 J to complete perforation. The samples impacted at 20 J at both temperatures experienced a combination of fiber fracture (enclosed by the red curves) and matrix cracking (enclosed by the blue curves). At 25 °C, these samples also manifested small regions of fiber bridging at the back face (enclosed by the green circles). On the other hand, at -50 °C, fiber bridging was minimal and showed predominantly fiber fracture at the back face of the laminate as predicted from the “Laminate Strengthening” section. This was also representative of the samples impacted at 25 J.

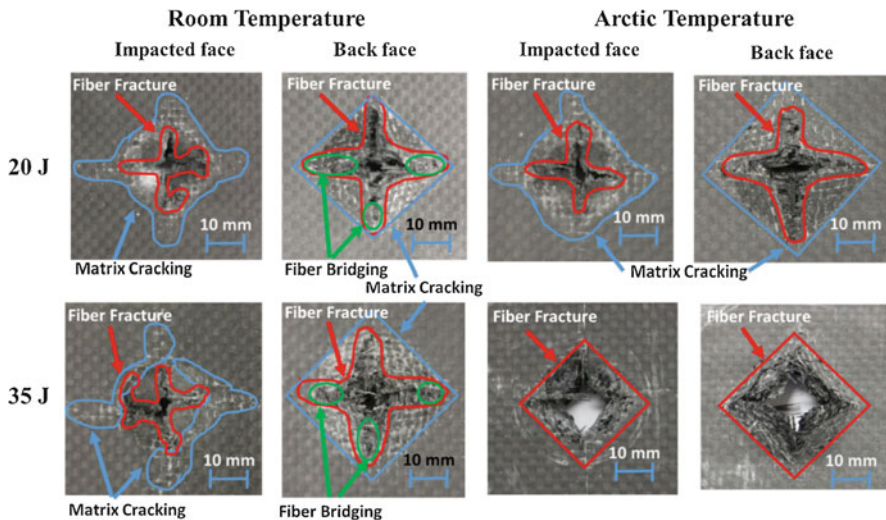


Fig. 17 Impacted face and back face for 20 J and 35 J impact energies at 25 °C and -50 °C under repeated impact

The samples impacted at 35 J at room temperature exhibited a combination of fiber breakage and matrix cracking along with fiber bridging at the back face of the laminate. On the other hand, at arctic temperature they experienced significant fiber fracture at the impacted and back face. The perforated region is sharp and well defined at 30 J in arctic temperature as compared to lower impact energies and at room temperature. The failure mechanisms were similar for the samples impacted at 30 J. Overall, arctic temperature renders the composite brittle thereby promoting more fiber fracture than matrix cracking, which is accentuated at higher impact energies.

4 Conclusion

Dynamic single and repeated impact response and failure mechanisms of woven carbon/vinyl ester composites at room (25 °C) and arctic (−50 °C) temperatures were investigated in this paper in view of increasing interest in arctic explorations and the need to characterize these composites for arctic applications. Four impact energies of 20 J, 25 J, 30 J and 35 J were considered for dynamic impact testing at room and in-situ arctic temperatures, where the samples were repeatedly impacted until perforation. Key observations in terms of the contact force, displacement, energy absorbed and failure mechanisms were reported in this paper. Key conclusions are summarized here.

Single Impact

- At −50 °C, the rigidity of the laminates increased due to resin strengthening that resulted in higher initial stiffness as compared to room temperature.
- Higher peak forces manifested in laminates impacted at −50 °C for all energies.
- Increased in strength also resulted in lower displacements in the laminates at −50 °C.
- The laminates absorbed less energy and correspondingly the degree of damage was lower at −50 °C than at 25 °C.
- At RT, the dominant failure mechanism was matrix failure (micro cracks/delamination) at low impact energies (20 J). Whereas, for higher impact energies (25 J, 30 J and 35 J), the dominant failure mechanism was fiber fracture along with considerable matrix failure.
- At AT, the overall damage area projected on to the plane of the composite reduced, however, manifested significantly higher fiber failure as compared to RT for the same impact energy, due to the brittleness of the sample at AT.
- The percentage reduction in damage area and the average degree of damage value between RT and AT exhibited a decreasing trend with increasing impact energies, as the influence of matrix failure is more dominant at lower impact energies and contribute higher to the extent of damage in a laminate.

Repeated Impact

- During a repeated impact event at low impact energies, a laminate experiences four phases of force change: stabilization, force increase, maximum force and force decrease. If the impact energy is sufficiently high to cause significant damage during the first impact, then only two phases of force change will be present: maximum force and force decrease.
- At $-50\text{ }^{\circ}\text{C}$, increase in rigidity of a laminate results in higher initial stiffness, lower deflections and higher impact forces than those impacted at $25\text{ }^{\circ}\text{C}$ for all energies.
- The laminates absorb less energy at $-50\text{ }^{\circ}\text{C}$ due to matrix strengthening, which results in lower values of degree of damage than at $25\text{ }^{\circ}\text{C}$. Consequently, the number of impacts needed for complete perforation of laminates increase at low temperature.
- At room temperature, the dominant failure mechanism is matrix cracking at low impact energies (20 J) as compared to higher impact energies (30 J and 35 J), where the dominant failure mechanism is fiber fracture with lesser matrix cracking.
- Significant shift in failure mechanisms occurs at arctic temperature, where fiber fracture is promoted due to matrix strengthening. This manifests as sharp defined perforated regions at low temperature with minimal fiber bridging at the back face of the laminate.
- Overall, the difference in response of laminates at lower energies is more distinct with temperature change from room to arctic, whereas, if velocity increases there will be a damage saturation effect where the temperature will have lower influence on the damage extension.

In conclusion, failure mechanisms shift from matrix failure towards fiber failure at arctic temperature, even though the measured degree of damage and deflection from the impact tests provide lower value at AT as compared to RT. This shift in mechanism can have significant detrimental effect on the tensile residual strength (as fiber fracture will be the main failure mechanism at AT) and durability of the composite. Also, this study is very relevant for developing appropriate repair techniques for composites for use in arctic applications.

Acknowledgments The author would like to acknowledge the partial support by the Department of Defense (DoD) Office of Naval Research – Young Investigator Program (ONR-YIP) Award [N00014-19-1-2206] and DoD HBCU/MI Basic Research Grant [W911NF-15-1-0430] for conducting the research presented here. The author would like to acknowledge the great amount of research work and input from Alejandra Castellanos, who has contributed significantly to the work presented here.

References

1. Abrate S (1994) Impact on laminated composites: recent advances. *Appl Mech Rev* 47:517–544
2. ASTM D3039M-17 (2017) Standard test method for tensile properties of polymer matrix composite materials. *J ASTM Int D3039M-17* 1–13

3. ASTM D695-15 (2015) Standard test method for compressive properties of rigid plastics. *J ASTM Int D695-15* 1–8
4. ASTM D7136/D7136M-15 (2015) Standard test method for measuring the damage resistance of a Fiber-reinforced polymer matrix composite to a drop-weight impact event. *J ASTM Int D7136/D7136M-15* 1–16
5. Babu S, Shivanand HK (2014) Impact analysis of laminated composite on glass Fiber and carbon Fiber. *Int J Emerg Technol Adv Eng* 4:824–829
6. Belingardi G, Vadori R (2003) Influence of the laminate thickness in low velocity impact behavior of composite material plate. *Compos Struct* 61:27–38
7. Bieniaś J, Surowska B, Jakubczak P (2015) Influence of repeated impact on damage growth in fibre reinforced polymer composites. *Maint Reliab* 17:194–198
8. Cantwell WJ, Morton J (1990) Impact perforation of carbon fibre reinforced plastic. *Compos Sci Technol* 38:119–141
9. Caprino V, Lopresto V, Scarponi C, Briotti G (1999) Effect of ZnO nanowire morphology on the interfacial strength of nanowire coated carbon Fibers. *Compos Sci Technol* 59:2279–2286
10. Chalmers DW (1994) The potential for the use of composite materials in marine structures. *Mar Struct* 7:441–456
11. Chittajallu K (2004) Computational modeling of the Vacuum Assisted Resin Transfer Molding (VARTM) process (master's thesis). Clemson University
12. Chu XX, Wu ZW, Huang RJ, Zhou Y, Li LF (2010) Mechanical and thermal expansion properties of glass fibers reinforced PEEK composites at cryogenic temperatures. *Cryogenics (Guildf)*. 50:84–88
13. Dempsey JP (2000) Research trends in ice mechanics. *Int J Solids Struct* 37:131–153
14. Dutta PK (1994) Low-temperature compressive strength of glass-fiber-reinforced polymer composites. *J Offshore Mech Arct Eng* 116:167–172
15. Garcia R, Castellanos AG, Prabhakar P (2019) Influence of arctic seawater exposure on the flexural behavior of woven carbon/vinyl ester composites. *J Sandw Struct Mater* 21(3):1190–1208. <https://doi.org/10.1177/1099636217710821>
16. Gibson AG (2003) The cost effective use of fibre reinforced compopsites offshore. *Rep Heal Saf Exec* 2003
17. Gomez-del-Rio T, Zaera R, Barbero E, Navarro C (2006) Damage in CFRPs due to low velocity impact at low temperature. *Compos Part B* 36:41–50
18. Greene E (1990) Use of Fiber reinforced plastics in the marine industry. *Home-Transport Res. Int Doc SSC-360*
19. Guedes Soares C, Garbatov Y (2017) *Progress in the analysis and Design of Marine Structures*. CRC Press/Balkema, London
20. Hartwig G, Knaak S (1984) Fibre-epoxy composites at low temperatures. *Cryogenics (Guildf)* 24:639–647
21. Ibekwe SI, Mensah PF, Li G, Pang SS, Stubblefield MA (2007) Impact and post impact response of laminated beam beams at low temperatures. *Compos Struct* 79:12–17
22. Icten BM (2014) Low temperature effect on single and repeated impact behavior of woven glass-epoxy composite plates. *J Compos Mater* 49:1171–1178
23. Im K, Cha C, Kim S, Yang I (2001) Effects of temperature on impact damages in CFRP composite laminates. *Compos Part B* 32:669–682
24. Jones N (1993) Recent studies on the response of structures Subected to large impact loads. *Soc Nav Archit Mar Eng Sh Struct Comm*:1–22
25. Julias A, Murali V (2014) Effect of carbon Fiber position on the impact behavior of glass/carbon Fiber hybrid composite laminates. *Int J Appl Eng Res* 9
26. Kim M, Kang S, Kim C, Kong C (2007) Tensile response of graphite/epoxy composites at low temperatures. *Compos Struct* 79:84–89
27. Li XK, Liu PF (2017) Expperimental analysis of low-velocity impact beaviors of carbon fibre composite laminates. *J Fail Anal Prev* 17:1126–1130

28. Lima Sobrinho L, Ferreira M, Bastian FL (2009) The effects of water absorption on an ester vinyl resin system. *Mater Res* 12:353–361
29. Lopez-Puente J, Zaera R, Navarro C (2002) The effect of low temperatures on the intermediate and high velocity impact response of CFRPs. *Compos Part B* 33:559–566
30. Morais WA, Monteiro SN, d'Almeida JRM (2009) Evaluation of repeated low energy impact damage in carbon-epoxy composite materials. *Compos Struct* 91:318–323
31. Murat BIS, Rahman AAA (2017) Study of impact damage behavior in woven carbon fiber plates. *Eng Phys Int Conf Epic* 2016:47–54
32. Naik NK, Chandreshakarkhar Y, Mduri S (2000) Polymer matrix woven fabric composites subjected to low velocity impact: part I. Damage initiation studies. *J Reinf Plast Compos* 19:912–943
33. Nguyen S, James T, L Iannucci (2016) Low, medium and high velocity impact on composites. 16th International Conference Composite Structures. 1–2
34. Rajkumar GR, Krishna M, Narasimha HN, Sharma SC, Vishnu KR (2012) Experimental investigation of low-velocity repeated impacts on glass fiber metal composites. *J Mater Eng Perform* 21:1485–1490
35. Safri SNA, Sultan MTH, Yidris N, Mustapha F (2014) Low velocity and high velocity impact test on composite materials – a review. *Int J Eng Sci* 3:50–60
36. Salehi-Khojin A, Bashirzadeh R, Mahinfalah M, Nakhaei-Jazar R (2006) The role of temperature on impact properties of Kevlar/fiberglass composite laminates. *Compos Part B* 37:593–602
37. Sayer M, Bektas NB, Sayman O (2010) An experimental investigation on the impact behavior of hybrid composite plates. *Compos Struct* 92:1256–1262
38. Selvaraju S, Illaiyavel S (2011) Application of composites in marine industry. *J Eng Res Stud* 2:89–91
39. Setvati MR, Shafiq N, Mustaffa X and Syed ZI (2014), A review on composite materials for offshore structures. in ASME. International conference on offshore mechanics and Arctic engineering 5, (ASME)
40. Shyr TW, Pan YH (2003) Impact resistance and damage characteristic of composite laminates. *Compos Struct* 62:193–203
41. Signor AW, Chin JW (2003) Effects of ultraviolet radiation exposure on vinyl ester matrix resins: chemical and mechanical characterization. *Polym Degrad Stab* 79:1–12
42. Sjoblom PO, Hartness JT, Cordell TM (1988) On low-velocity impact testing of composite materials. *Compos Mater* 22:30–52
43. Sultan MT, Worden K, Staszewski WJ, Hodzic A (2012) Impact damage characterization of composite laminates using a statistical approach. *Compos Sci Technol* 72:1108–1120
44. Szekrényes A (2002) Overview on the experimental investigations of the fracture toughness in composite materials. *Hungarian Electron J Sci*:1–19
45. Wang XF, Zhao JH (2001) Monte-Carlo simulation to the tensile mechanical behaviors of unidirectional composites at low temperature. *Cryogenics (Guildf)* 41:683–691
46. Yusriah L, Mariatti M, Bakar AA (2010) The properties of vinyl ester composites reinforced with different types of woven fabric and hollow phenolic microspheres. *J Reinf Plast Compos* 29:3066–3073
47. Zhu L, Faulkner D (1996) Damage estimate for plating of ships and platforms under repeated impacts. *Mar Struct* 9:697–720